Evidences of Conformal Invariance in 2D Rigidity Percolation

Nina Javerzat[1,*] and Mehdi Bouzid[2,†]
[1]SISSA and INFN Sezione di Trieste, via Bonomea 265, 34136, Trieste, Italy
[2]Université Grenoble Alpes, CNRS, Grenoble INP, 3SR, F-38000, Grenoble, France

(Received 11 October 2022; revised 4 February 2023; accepted 10 May 2023; published 28 June 2023)

The rigidity transition occurs when, as the density of microscopic components is increased, a disordered medium becomes able to transmit and ensure macroscopic mechanical stability, owing to the appearance of a space-spanning rigid connected component, or cluster. As a second-order phase transition it exhibits a scale invariant critical point, at which the rigid clusters are random fractals. We show, using numerical analysis, that these clusters are also conformally invariant, and we use conformal field theory to predict the form of universal finite-size effects. Furthermore, although connectivity and rigidity percolation are usually thought to be of fundamentally different natures, we provide evidence of unexpected similarities between the statistical properties of their random clusters at criticality. Our work opens a new research avenue through the application of the powerful 2D conformal field theory tools to understand the critical behavior of a wide range of physical and biological materials exhibiting such a mechanical transition.

DOI: 10.1103/PhysRevLett.130.268201

Introduction.—Symmetries are the cornerstone to understand and to model physical phenomena [1] and their identification, a powerful guiding principle for deriving physical laws. Indeed, the compatibility between symmetries often results in constraints on the physical properties of the system: for example, the compatibility of discrete translations and rotations in crystals leads to the crystallographic restriction theorem, which classifies all patterns of periodic discrete lattices one can encounter in nature [2]. However, symmetries are not only deterministic: second-order phase transitions are a paradigmatic example of systems possessing a random symmetry, where the long-range statistical fluctuations are invariant in law under change of scale. For a host of systems exhibiting critical behavior—as diverse as linear polymers [3], graphene membranes [4], and disordered systems [5]—a larger symmetry emerges and fluctuations are also invariant under local rescalings, i.e., under all geometrical transformations that preserve angles and rescale distances, called conformal transformations [6]. The emergence of this enhanced symmetry is a powerful tool: exploiting the compatibility constraints on the physical observables allows us to understand and predict the universal features of phase transitions [7] and even, in some cases, to fully characterize the scaling limit [8]. Conformal invariance has also been successful in establishing deep connections between apparently unrelated critical phenomena, e.g., in turbulence [9,10] and in nonequilibrium growth processes [11–13]. The origin of conformal symmetry is, however, still not systematically understood [14], even in two dimensions. Indeed, while in 2D unitary systems conformal invariance is automatically implied by scale invariance [15,16], this is not true anymore for nonunitary phenomena, of which percolation is maybe the most representative and versatile example. Still, percolation in its various forms (Bernoulli percolation [17], the random Q-states Potts model [18], percolation of random surfaces [4,19], etc.) is conformally invariant, and to our knowledge there is no equilibrium percolation model that has been shown to be scale, but not conformal, invariant.

In this context, rigidity percolation (RP) is an ideal model to study the possible emergence of conformal symmetry. Indeed, on the one hand, it is the first time that conformal invariance is studied in a percolation phenomenon of mechanical nature [*a priori* distinct from the "connectivity percolation" (CP) models mentioned above], and this might shed some light on which features of a percolation model make its scaling limit conformally invariant. On the other hand, establishing the conformal invariance of this second-order phase transition, of prominent importance in soft matter, may allow us to better characterize its still poorly known universality class. Rigidity percolation in central force random springs models indeed provides a generic theoretical and simple framework to study how a system transitions from a liquid to a solid phase, where the underlying building blocks assemble into a percolating cluster, able to transmit stresses to the boundary and sustain external loads. It has been successfully used to highlight the structural and mechanical properties of many soft materials, such as living tissues [20], biopolymer networks [21,22], molecular glasses [23], stability of granular packings [24–26], or colloidal gelation [27–29]. Several critical exponents, characterizing the long-distance critical behavior, have been numerically determined, such as the correlation length exponent $\nu = 1.21 \pm 0.06$ and the order parameter exponent $\beta = 0.18 \pm 0.02$, defining an *a priori* new universality class [30]. Hyperscaling

relations also give the fractal dimension of the rigid cluster as $d_f = 2 - \beta/\nu = 1.86 \pm 0.02$, a value that was confirmed by direct measurement [27].

In this Letter, we show that (i) the rigidity percolation clusters exhibit conformal invariance right at the critical point, (ii) we use conformal field theory to predict the form of universal finite-size effects and, interestingly, find that (iii) the fine statistical properties of the RP clusters and of the CP clusters share surprising similarities, despite belonging to distinct universality classes.

Model and methods.—We perform three independent numerical tests to show conformal invariance, based on the study of a standard geometrical observable of percolation clusters, their so-called n-point connectivity [31],

$$p_{12,\ldots,n}(z_1,\ldots,z_n) \overset{\text{def}}{=} \text{Prob}[z_1,\ldots,z_n \in \mathcal{RC}], \qquad (1)$$

where z_i are points in the plane and $\mathcal{RC}$ denotes a rigid cluster. Equation (1) gives therefore the probability that n points are connected by paths inside the same rigid cluster. These quantities have been very useful to understand connectivity percolation [32–36]. We make the central assumption that, in the scaling limit, the connectivities (1) can be described by a field theory and, more precisely, that they are given by correlation functions of a scaling field that we denote Φ_c, of scaling dimension Δ_c [37],

$$p_{12,\ldots,n}(z_1,\ldots,z_n) \underset{\text{lim}}{\overset{\text{scaling}}{\longrightarrow}} a_0^{(n)} \langle \Phi_c(z_1) \cdots \Phi_c(z_n) \rangle, \qquad (2)$$

where $a_0^{(n)}$ is a nonuniversal constant that depends on the microscopic details of the model. Our tests rely on the fact that, if the percolation model under study is conformally invariant, the form of the correlation functions (2) is constrained in a precise way, which can be derived from conformal field theory (CFT). We use a lattice model of rigidity percolation to measure numerically the rigid cluster connectivities (1) on specific geometries. Comparing their scaling limit to the corresponding CFT predictions, we conclude about the conformal invariance of RP clusters.

The model is a site-diluted triangular lattice with local spatial correlations. It has been recently introduced to model the rigidity percolation of soft solids [27]. At each step, particles are drawn randomly one by one to populate a doubly periodic triangular lattice of size $L_1 \times L_2$ ($L_1 \geq L_2$), according to the following probability $p = (1-c)^{6-N_n}$, where $0 \leq c < 1$ represents the degree of correlation and N_n is the number of occupied nearest neighbors. $c = 0$ corresponds to the uncorrelated case and for $c \neq 0$ the introduced correlations are local, since the filling probability depends only on the occupation of the first neighbors. They are therefore irrelevant to the large-scale behavior, so that the transition for $c > 0$ belongs to the same universality class as uncorrelated RP [27]. In practice, the larger the c, the smallest the critical probability threshold p_c^{RP}; we take $c = 0.3$, at which

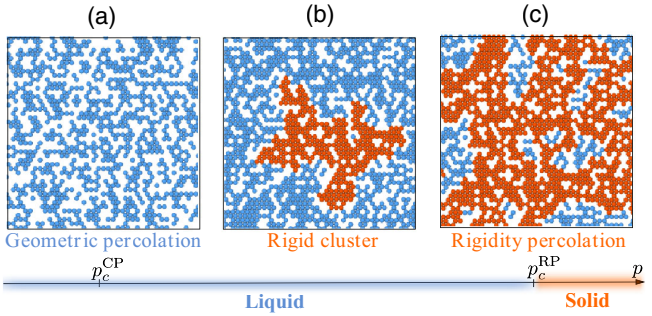

FIG. 1. Examples of lattice configurations showing (a) the connectivity percolation transition at p_c^{CP}, (b) the largest rigid cluster at $p_c^{\text{CP}} < p < pc^{\text{RP}}$, and (c) the rigidity percolation transition at p_c^{RP}.

$p_c^{\text{RP}}(c = 0.3) \sim 0.66$. To identify rigid clusters on a discrete lattice, we use the so-called pebble game, a fast combinatorial algorithm [30,38], based on Laman's theorem for a graph's rigidity [39], which uses Maxwell's constraint counting argument to detect overconstrained clusters. Figure 1 shows an example of cluster decomposition while increasing p. Connectivity percolation arises at p_c^{CP} and is characterized by a space-spanning percolating cluster (in blue). The system is macroscopically liquid and cannot sustain external loads. Figures 1(b) and 1(c) show the largest rigid cluster (in red) that percolates at $p_c^{\text{RP}} > p_c^{\text{CP}}$, leading to macroscopic elasticity.

In the following, we analyze the statistical structural properties of the rigid clusters right at the critical point. We first obtain a direct measurement of the anomalous dimension exponent η, then move on to test conformal invariance, using the three- and two-point connectivities. Finally, we highlight the similarities of these observables in CP and RP.

Anomalous dimension.—We measure the two-point connectivity $p_{12}(r,\theta)$ on the lattice, i.e., the probability that points (i,j) and $(i + r\cos(\theta + \pi/3), j + r\sin(\theta + \pi/3))$ are in the same rigid cluster. θ is the angle with respect to the short cycle of the doubly periodic lattice, and r is the distance between the two points. We use translation invariance to average over the $L_1 \times L_2$ positions (i,j), as well as symmetry by reflection about $\theta = 0$, so that p_{12} is an average over $2L_1L_2N$ measurements with N the number of samples ($N = 1200$ for the largest sizes). The inset in Fig. 3 shows the data points in log-log scale, which follow a power law in the scaling region $1 \ll r \ll L_2/2$ as expected from scale invariance: the two-point connectivity decays as $p_{12}(z_1,z_2) \sim |z_{12}|^{-\eta}$, where η is the so-called anomalous dimension, satisfying the hyperscaling relations $\eta = 2\beta/\nu = 4 - 2d_f$ [40]. Using assumption (2) and the scale invariance property $\langle \Phi_c(z_1)\Phi_c(z_2) \rangle = z_{12}^{-2\Delta_c}$ [41] gives the scaling dimension of Φ_c as $\Delta_c = \eta/2$. Expected deviations in the region $r \sim L_2/2$ are due to universal finite-size effects coming from the doubly periodic boundary conditions. Fitting the data points

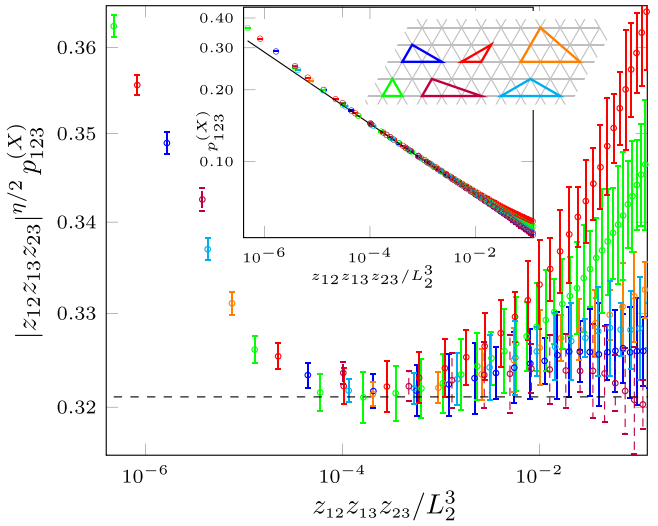

FIG. 2. Rescaled three-point connectivity measured on the six inequivalent triangles shown in the inset, on a 384×128 lattice. Inset: unrescaled three-point connectivity; the black line has slope $\eta/2$.

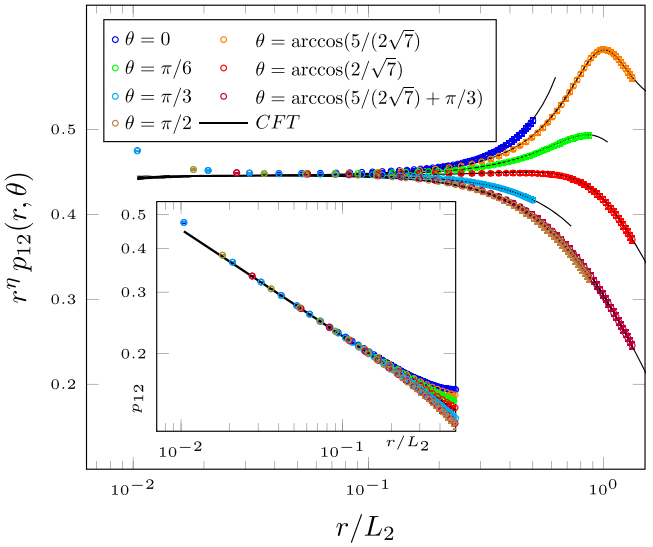

FIG. 3. Rescaled two-point connectivity measured on a 576×96 lattice along different angles. The black curves give the CFT prediction (4). Inset: same data points, not rescaled, in log-log scale. The black line has slope $\eta = 0.307$.

corresponding to the angle that minimizes such effects [$\theta = \arccos[2/\sqrt{7}]$] we obtain the value of the nonuniversal constant $a_0^{(2)} = 0.448 \pm 0.002$ and of the anomalous dimension $\eta = 0.307 \pm 0.002$, in agreement with the values of the critical exponents in the literature [30] via hyperscaling.

Global conformal invariance.—In two dimensions, conformal transformations are all the analytic maps of the Riemann sphere (complex plane plus point at infinity). They can be distinguished into a finite set of globally defined (everywhere invertible) transformations (translation, rotation, scaling, special conformal transformation) and an infinite set of local transformations [41]. It is a standard result that imposing invariance under the global transformations fixes completely the form of three-point correlations, so that, using (2), one expects the three-point connectivity of globally invariant clusters to be [41]

$$p_{123}(z_1, z_2, z_3) = a_0^{(3)} \frac{C_{\Phi_c\Phi_c}^{\Phi_c}}{|z_{12}z_{23}z_{13}|^{\eta/2}}, \tag{3}$$

where $C_{\Phi_c\Phi_c}^{\Phi_c}$ is an universal constant called operator product expansion (OPE) coefficient [42]. In Fig. 2, we show the connectivity (inset) and the rescaled connectivity measured on six inequivalent configurations of points, as a function of $|z_{12}z_{13}z_{23}|/L_2^3$. In the scaling region, a clear collapse of the data points is observed (inset), while the rescaled connectivity tends to a configuration-independent constant (dashed line), showing the validity of (3). Microscopic and configuration-dependent finite-size effects dominate at small and large separation, respectively.

Local conformal invariance.—We now use the universal finite-size effects induced by the torus geometry (also known as periodic boundary condition) to probe the local conformal invariance. In particular, we put the system on a cylinder, conformally equivalent to the plane through the map $z \to iL_2/2\pi \log z$. For a CFT, the expression of a two-point correlation function on this geometry is a well-known result [41] and in polar coordinates it reads

$$p_{12}(r,\theta) = \frac{a_0^{(2)}(2\pi/L_2)^\eta}{[2\cosh(\frac{2\pi}{L_2} r\cos\theta) - 2\cos(\frac{2\pi}{L_2} r\sin\theta)]^{\eta/2}}. \tag{4}$$

This prediction is drawn in Fig. 3 for different angles θ, using the values of η and $a_0^{(2)}$ found previously, along with the corresponding numerical data points measured on a torus with large aspect ratio $L_1/L_2 = 6$ to reproduce the cylinder limit. The remarkable agreement confirms that the two-point connectivity of rigid clusters transforms correctly under this local conformal transformation. In more technical terms, the data are consistent with the connectivity field Φ_c being a Virasoro primary, so that one can expect all connectivities to be conformally invariant as well.

Finite-size corrections and comparison with CP.—On a torus of finite aspect ratio, one can write generically a so-called OPE expansion [42], for $r \ll L_2$, of the two-point connectivity as [43]

$$\frac{r^\eta p_{12}(r,\theta)}{a_0^{(2)}} = \sum_{\Phi_\alpha} C_{\Phi_c\Phi_c}^{\Phi_\alpha} \langle\Phi_\alpha\rangle_q (2 - \delta_{s_\alpha,0}) \cos(s_\alpha\theta) \left(\frac{r}{L_2}\right)^{\Delta_\alpha}. \tag{5}$$

The sum is a (potentially infinite) sum over an *a priori* unknown set of fields Φ_α with dimension Δ_α and spin $s_\alpha \geq 0$. Each field contribution gives a r/L_2 correction of order Δ_α

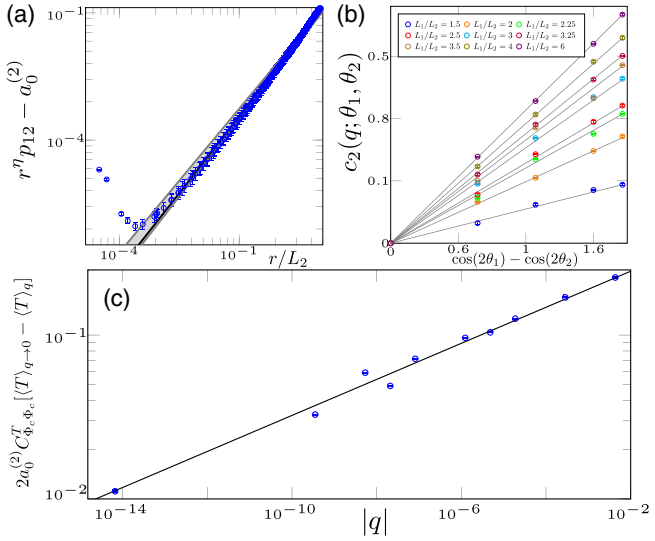

FIG. 4. (a) Dominant finite-size effects: data points are obtained on a 256×256 lattice. The line gives the best fit corresponding to $\nu = 1.19 \pm 0.01$. The gray area corresponds to ν in the confidence interval of [30]. (b) Coefficients c_2 for different aspect ratios. The gray lines are best fits, whose slopes give the points of (c). (c) Behavior of $\langle T\rangle_q$ with q, the line gives the fit $\sim|q|^{0.11}$.

to the plane limit (corresponding to $\Delta_\alpha = 0$), encoding the universal finite-size effects. They depend on the elliptic nome of the torus $q = e^{-2\pi L_1/L_2 \sin\pi/3} e^{2\pi i L_1/L_2 \cos\pi/3}$, through the expectation value $\langle\Phi_\alpha\rangle_q$, and on θ for nonscalar fields which have $s_\alpha > 0$. On a square torus ($L_1 = L_2$), p_{12} is independent of θ and $\langle\Phi_\alpha\rangle_q$ must vanish for nonscalar fields. We find that, for RP, the first terms in expansion (5) are the following:

$$\frac{r^\eta p_{12}(r,\theta)}{a_0^{(2)}} = 1 + C^{\Phi_\nu}_{\Phi_c\Phi_c}\langle\Phi_\nu\rangle_q \left(\frac{r}{L_2}\right)^{2-1/\nu} + 2C^T_{\Phi_c\Phi_c}\langle T\rangle_q \cos(2\theta)\left(\frac{r}{L_2}\right)^2 + \cdots. \tag{6}$$

The dominant finite-size correction is given by the "thermal" field Φ_ν of dimension $\Delta_\nu = 2 - 1/\nu$, and the first nonscalar contribution comes from the so-called stress-energy tensor T. This latter field is the tensor of conserved currents and from dimensional analysis has dimension 2 and spin 2. The dots account for the higher-order unknown contributions. In Fig. 4(a), we show the dominant finite-size correction: by measuring p_{12} on a square torus, we eliminate the nonscalar contributions to (6), so that $r^\eta p_{12} - a_0^{(2)}$ is directly proportional to the dominant scalar contribution, up to subleading corrections. The gray area corresponds to a term $\sim(r/L_2)^{2-1/\nu}$ with ν in the confidence interval of [30], $\nu = 1.21 \pm 0.06$. Fitting in the range $1 \ll r \ll L_2/2$ gives $\nu = 1.19 \pm 0.01$.

The dominant nonscalar field contribution is instead obtained by measuring p_{12} in two directions θ_1, θ_2 to cancel the scalar terms and is consistent with a dimension-two field, namely,

$$r^\eta[p_{12}(r,\theta_1) - p_{12}(r,\theta_2)] = \underbrace{a_0^{(2)} 2C^T_{\Phi_c\Phi_c}\langle T\rangle_q[\cos(2\theta_1) - \cos(2\theta_2)]}_{\equiv c_2(q;\theta_1,\theta_2)}\left(\frac{r}{L_2}\right)^2 + \cdots. \tag{7}$$

We extracted the order-two coefficients $c_2(q;\theta_1,\theta_2)$ of $r^\eta[p_{12}(r,\theta_1) - p_{12}(r,\theta_2)]$, measured for different aspect ratios and different angles, and plotted them in Fig. 4(b) as a function of $\cos(2\theta_1) - \cos(2\theta_2)$. The straight lines confirm that we are measuring the contribution of a dimension-two and spin-two field, i.e., of T. From (7) their slopes correspond to $a_0^{(2)} 2C^T_{\Phi_c\Phi_c}\langle T\rangle_q$ and are plotted as a function of the elliptic nome q in Fig. 4(c). Fitting these points, we find that

$$\langle T\rangle_{q\to 0} - \langle T\rangle_q \sim |q|^{\Delta_0}, \qquad \Delta_0 \sim 0.11. \tag{8}$$

First, this form is consistent with CFT, which gives $\langle T\rangle_q$ as [41]

$$\langle T\rangle_q = -(2\pi)^2 q\partial_q \log Z(q), \tag{9}$$

where $Z(q)$ is the partition function on the torus, $Z(q) \equiv \sum_{\Phi_\alpha} n_\alpha q^{(\Delta_\alpha + s_\alpha)/2 - c/24}\bar{q}^{(\Delta_\alpha - s_\alpha)/2 - c/24}$, with c as the so-called central charge—an important parameter characterizing a CFT—and n_α as the multiplicity of field Φ_α. Equation (9) is one of the most direct consequences, at the level of observables, of conformal invariance, coming from the holomorphicity of T ($\bar\partial T = 0$). Expanding for small q gives

$$\langle T\rangle_q \overset{q\ll 1}{\sim} (2\pi)^2\left[\frac{c}{24} - n_0\frac{\Delta_0}{2}|q|^{\Delta_0} + \cdots\right]. \tag{10}$$

The constant term corresponds to the cylinder limit $\langle T\rangle_{q\to 0} = (2\pi)^2 c/24$. From (8) the value of the smallest dimension Δ_0 in (10) is compatible with the scaling dimension of Φ_c, $\Delta_c = \eta/2 = 0.15 \pm 0.02$ and so compatible with the connectivity field Φ_c being the field with smallest nonzero dimension in the theory.

It has been established that the expansion (6) of the torus two-point connectivity holds in correlated CP models (the Q-state Potts model [43], percolation of random surfaces [19]), namely, that the dominant terms in the $\Phi_c \times \Phi_c$ OPE are the conformal families of the identity and thermal fields. For these models, it was also found that the field with smallest scaling dimension entering the partition function is the connectivity field. Therefore, our results indicate that, within our numerical range, the structures of the OPE and of the partition function are identical for RP and CP.

In other words, at the level of random clusters, we find no more difference between RP and CP than between two different CP universality classes. In this respect, it would be useful to characterize more precisely the CFT of RP clusters by determining, in particular, its central charge c. These data are not accessible in our study as it cancels in (7), given that $C^T_{\Phi_c\Phi_c} = \Delta_c/c$ [44].

Conclusion.—In this Letter, we have investigated a second-order rigidity percolation transition. Through a series of three original and independent tests, we have shown—for the first time—that the statistical properties of the critical random clusters, encoded in the connectivity functions, are conformally invariant and that the universal finite-size effects can be predicted by CFT. These results hold independent of the nature of the microscopic details, provided that the model belongs to the same universality class. Given that RP exhibits highly nonlocal interactions, where the removal of a single bond might destroy the rigidity of an arbitrary large region, it is quite remarkable that invariance under local rescalings holds and that one can predict the cluster's connectivities using correlations of local fields. We can presume that conformal symmetry remains unbroken for rigidity transitions arising in gel-like systems [28,29,45], granular media [25,46], biological tissues [20], or subisostatic biopolymer networks where the emergence of such a transition is driven by external deformations [47,48]. Surprisingly, we found that the structure of the connectivities in RP and CP are identical, albeit with *a priori* different values of the universal data (critical exponents and OPE coefficients). Therefore, although it is widely believed that the rigidity and the connectivity percolation phenomena are of fundamentally different natures, our Letter provides evidences of the similarity of their clusters at criticality. These findings support the suggestion of [49], that the geometrical properties of rigidity might be physically independent from the elastic properties. Recent work on RP for granular media near the jamming transition [46] also points toward a possible superuniversality of RP and CP critical exponents.

Many questions remain open, in particular, concerning the relations between structural properties and mechanical response. Indeed, away from the transition, growing evidence points toward universal features for the stress propagation in gels and granular media [50], and recent field theories have been very successful in predicting the elastic response of disordered amorphous materials [51,52]. The vicinity of the transition remains much less understood. Whether signatures of conformal invariance can be found, e.g., in the stress propagation at the verge of rigidity, remains a tantalizing possibility that may open a new avenue of thinking to build a unified framework to describe the mechanical properties of a wide range of materials, right at and close to their mechanical stability.

The authors thank Alexandre Nicolas, Filiberto Ares, Xiaoming Mao, Emanuela Del Gado, Ezequiel Ferrero, and Gesualdo Delfino for insightful discussions, as well as Raoul Santachiara who suggested this problem to us. N. J. acknowledges support from ERC under Consolidator Grant No. 771536 (NEMO).

*njaverza@sissa.it
†mehdi.bouzid@univ-grenoble-alpes.fr

[1] D. J. Gross, Proc. Natl. Acad. Sci. U.S.A. **93**, 14256 (1996).
[2] C. Giacovazzo, C. Giacovazzo, H. L. Monaco, G. Artioli, D. Viterbo, M. Milanesio, G. Gilli, P. Gilli, G. Zanotti, G. Ferraris, and M. Catti, *Fundamentals of Crystallography* (Oxford University Press, New York, 2011).
[3] H. Saleur, J. Phys. A **20**, 455 (1987).
[4] I. Giordanelli, N. Posé, M. Mendoza, and H. J. Herrmann, Sci. Rep. **6**, 22949 (2016).
[5] G. Delfino, Eur. Phys. J. B **94**, 65 (2021).
[6] A. M. Polyakov, JETP Lett. **12**, 381 (1970), http://jetpletters.ru/ps/1737/article_26381.shtml.
[7] D. Poland and D. Simmons-Duffin, Nat. Phys. **12**, 535 (2016).
[8] A. A. Belavin, A. M. Polyakov, and A. B. Zamolodchikov, Nucl. Phys. **B241**, 333 (1984).
[9] D. Bernard, G. Boffetta, A. Celani, and G. Falkovich, Nat. Phys. **2**, 124 (2006).
[10] J. Cardy, Nat. Phys. **2**, 67 (2006).
[11] A. A. Saberi and S. Rouhani, Phys. Rev. E **79**, 036102 (2009).
[12] A. A. Saberi, H. Dashti-Naserabadi, and S. Rouhani, Phys. Rev. E **82**, 020101(R) (2010).
[13] X. Cao, A. Rosso, and R. Santachiara, Europhys. Lett. **111**, 16001 (2015).
[14] Y. Nakayama, Phys. Rep. **569**, 1 (2015).
[15] J. Polchinski, Nucl. Phys. **B303**, 226 (1988).
[16] A. B. Zamolodchikov, Pis'ma Zh. Eksp. Teor. Fiz. **43**, 565 (1986), http://jetpletters.ru/ps/1413/article_21504.shtml.
[17] S. Smirnov, C.R. l'Acad. Sci. Ser. I **333**, 239 (2001).
[18] S. Smirnov, arXiv:0708.0032.
[19] N. Javerzat, S. Grijalva, A. Rosso, and R. Santachiara, SciPost Phys. **9**, 050 (2020).
[20] N. I. Petridou, B. Corominas-Murtra, C.-P. Heisenberg, and E. Hannezo, Cell **184**, 1914 (2021).
[21] C. P. Broedersz, X. Mao, T. C. Lubensky, and F. C. MacKintosh, Nat. Phys. **7**, 983 (2011).
[22] X. Mao, A. Souslov, C. I. Mendoza, and T. C. Lubensky, Nat. Commun. **6**, 5968 (2015).
[23] M. Thorpe, D. Jacobs, M. Chubynsky, and J. Phillips, J. Non-Cryst. Solids **266**, 859 (2000).
[24] S. Feng, Phys. Rev. B **32**, 510 (1985).
[25] S. Henkes, D. A. Quint, Y. Fily, and J. M. Schwarz, Phys. Rev. Lett. **116**, 028301 (2016).
[26] E. Berthier, J. E. Kollmer, S. E. Henkes, K. Liu, J. M. Schwarz, and K. E. Daniels, Phys. Rev. Mater. **3**, 075602 (2019).
[27] S. Zhang, L. Zhang, M. Bouzid, D. Z. Rocklin, E. Del Gado, and X. Mao, Phys. Rev. Lett. **123**, 058001 (2019).
[28] J. Rouwhorst, C. Ness, S. Stoyanov, A. Zaccone, and P. Schall, Nat. Commun. **11**, 3558 (2020).

[29] H. Tsurusawa, M. Leocmach, J. Russo, and H. Tanaka, Sci. Adv. **5**, eaav6090 (2019).
[30] D. J. Jacobs and M. F. Thorpe, Phys. Rev. Lett. **75**, 4051 (1995).
[31] G. Grimmett, *Percolation* (Springer, Berlin, Heidelberg, 1999), Chap. 6.
[32] G. Delfino and J. Viti, J. Phys. A **44**, 032001 (2010).
[33] M. Picco, S. Ribault, and R. Santachiara, SciPost Phys. **1**, 009 (2016).
[34] J. L. Jacobsen and H. Saleur, J. High Energy Phys. 01 (2019) 084.
[35] Y. He, J. L. Jacobsen, and H. Saleur, J. High Energy Phys. 01 (2020) 019.
[36] N. Javerzat, S. Grijalva, A. Rosso, and R. Santachiara, SciPost Phys. **9**, 050 (2020).
[37] J. Cardy, in Exact methods in low-dimensional statistical physics and quantum computing, *Proceedings of the Les Houches Summer School, Session LXXXIX* (Oxford University Press, Oxford, 2010), p. 65.
[38] D. J. Jacobs and M. F. Thorpe, Phys. Rev. E **53**, 3682 (1996).
[39] G. Laman, J. Eng. Math. **4**, 331 (1970).
[40] D. Stauffer and A. Aharony, *Introduction to Percolation Theory* (Oxford University Press, New York, 1971).
[41] P. Di Francesco, P. Mathieu, and D. Senechal, *Conformal Field Theory* (Springer-Verlag, New York, 1997).
[42] J. L. Cardy, *Scaling and Renormalization in Statistical Physics* (Cambridge University Press, 1996), Chap. 5.
[43] N. Javerzat, M. Picco, and R. Santachiara, J. Stat. Mech. (2020) 023101.
[44] N. Javerzat, New conformal bootstrap solutions and percolation models on the torus, Ph.D. Thesis, Université Paris-Saclay, 2020.
[45] M. Bantawa, B. Keshavarz, M. Geri, M. Bouzid, T. Divoux, G. H. McKinley, and E. Del Gado, arXiv:2211.03693.
[46] K. Liu, S. Henkes, and J. M. Schwarz, Phys. Rev. X **9**, 021006 (2019).
[47] A. Sharma, A. Licup, K. Jansen, R. Rens, M. Sheinman, G. Koenderink, and F. MacKintosh, Nat. Phys. **12**, 584 (2016).
[48] J. L. Shivers, S. Arzash, A. Sharma, and F. C. MacKintosh, Phys. Rev. Lett. **122**, 188003 (2019).
[49] D. A. Head, F. C. MacKintosh, and A. J. Levine, Phys. Rev. E **68**, 025101(R) (2003).
[50] H. Vinutha, F. D. Diaz Ruiz, X. Mao, B. Chakraborty, and E. Del Gado, J. Chem. Phys. **158**, 114104 (2023).
[51] E. DeGiuli, Phys. Rev. Lett. **121**, 118001 (2018).
[52] J. N. Nampoothiri, Y. Wang, K. Ramola, J. Zhang, S. Bhattacharjee, and B. Chakraborty, Phys. Rev. Lett. **125**, 118002 (2020).